ARCHIVES OF ELECTRICAL ENGINEERING VOL. 69(4), pp. 907–920 (2020)

DOI 10.24425/aee.2020.134638

A self-scheduling strategy of virtual power plant with electric vehicles considering margin indexes

FENGSHUN JIAO[1], YONGSHENG DENG[1], DUO LI[1], BO WEI[1], CHENGYAN YUE[2], MENG CHENG[2], YAPENG ZHANG[2], JIARUI ZHANG[2]

[1] *China Southern Power Grid Shenzhen Power Supply Bureau Co. LTD*
Shenzhen, China

[2] *ABB Power Grids Investment (China) Limited*
Beijing, China
e-mail: fsunjiao@163.com

(Received: 15.02.2020, revised: 09.07.2020)

Abstract: From the perspective of a virtual power plant (VPP) with electric vehicles (EVs), a self-scheduling strategy considering the response time margin (RTM) and state of charge margin (SOCM) is proposed. Firstly, considering the response state of the state of charge (SOC) and charge-discharge state of EVs, a VPP based response capacity determination model of EVs is established. Then, RTM and SOCM indexes are introduced on the basis of the power system scheduling target and the EV users' traveling demands. The RTM and SOCM indices are calculated and then are used to generate a priority sequence of responsive EVs for the VPP. In the process of the scheduling period and rolling iteration, the scheduling schemes of the EVs in the VPP for multiple time periods are determined. Finally, the VPP self-scheduling strategy is validated by taking an VPP containing three kinds of EV users as an example. Simulation results show that with the proposed strategy, the VPP is able to respond to the scheduling power from the power system, while ensuring the traveling demands of the EV users at the same time.

Key words: electric vehicle (EV), response time margin (RTM), scheduling strategy, state of charge margin (SOCM), virtual power plant (VPP)

1. Introduction

With the increasing depletion of fossil energies, the world is confronted with a huge challenge of energy shortage and environmental pollution issues [1]. At the end of the 20th century, the wide attention on the environmental protection promoted the energy technology revolution represented

by the renewable generation in energy production [2]. Meanwhile, the expectation of green, clean and efficient energy consumption has also given rise to the booming development of electric vehicles (EVs). According to the statistical data of the EV market, the number of EVs in China is expected to reach 60 million by 2030 [3].

For the EVs, the vehicle-to-grid (V2G) technology refers to a bi-directional power flow between the EV and the power system, and it can increase the flexible response regulation capability of EVs [4, 5]. Considering the limited response capacity of a single EV [6], the EVs are usually grouped into a virtual power plant (VPP) to participate in the system operation by adjusting the power exchange with the power grid according to a priority sequence [7, 8]. Similar to the conventional power plants, the VPP is an aggregator of EVs. The VPP can provide stable power regulation service to the power system. The state of charge (SOC) is usually used as an indicator for avoiding the over-charge or over-discharge of an EV battery. However, due to the small capacity of a single EV battery, participating in the scheduling operation of a power system for a continuous time period will lead to the SOC variation. This will have a non-negligible impact on its responsiveness at the subsequent time periods, and ultimately prevent the VPP from formulating an effective scheduling resource for the power systems [9, 10].

At present, there are two main types of research on the scheduling strategy of the EV charging loads at the demand side, including *centralized control* and *decentralized control*. The centralized control formulates a unified charging and discharging strategy for the EVs in the VPP. In [11], based on the genetic algorithm with the objective of reducing the EV charging load fluctuations, a charging and discharging strategy for the VPP with large-scale EVs was established. In [12], a unified power regulation strategy based on power flow tracing was developed for the unit commitment of wind farms using the EVs. To schedule real-time power control for EVs with the aggregated EV model, the SOC-based sorting algorithm [13], the least laxity first algorithm [6], and the optimization algorithm [14] were used by a central operator to update the power exchange of individual EVs. However, the centralized control strategy is usually unable to give a specific control scheme to individual EVs in the VPP. It may cause inadequate response capability or second disturbance to the power system [15–17]. Therefore, it is necessary to develop a series of decentralized control strategies to meet the actual needs of VPPs. For this reason, a multi-time-scale hierarchical control algorithm of EVs was developed in [18]. The researchers in [13] proposed a frequency response control strategy of EVs considering traveling behaviors of EV users in a decentralized way. The decentralized control allows individual EVs to determine their own charging and discharging preferences, and intelligent devices should be applied to schedule EVs' charging and discharging processes [19, 20].

However, the above studies ignored the influence of the SOC changes of an EV battery. The influence of the charging and discharging state on the response capacity of the VPP after power scheduling is not fully considered. Actually, the change of the above states is closely related to the scheduling strategy of the VPP. In order to solve the above problems, a self-scheduling strategy considering the response time margin (RTM) and state of charge margin (SOCM) is proposed. Simulation results show that with this proposed strategy, the VPP is able to respond to the scheduling power from the power system effectively in a continuous way. At the same time, the proposed strategy ensures the traveling demands of EV users.

2. Framework

The self-scheduling strategy of a VPP has three levels:

1. Control center level;
2. VPP level;
3. Individual EV level.

The framework of the VPP scheduling with EVs is shown in Fig. 1.

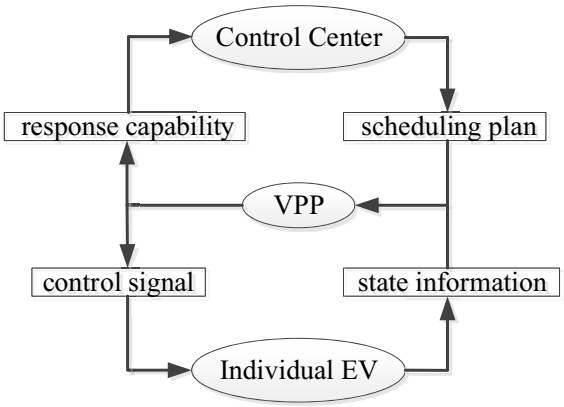

Fig. 1. Framework of the VPP scheduling with EVs

At the Control center level, the scheduling scheme is determined considering several increasingly important factors such as load uncertainties, unit outage and the variation of renewable power, as they are massively integrated into power grids. The scheduling scheme is then issued to the VPP within its available response capacity for the regulation of the power system. The scheduling scheme at this level is given by the system operators instead of being considered in detail in this paper.

At the VPP level, the scheduling scheme issued by the control center is allocated to each EV using the self-scheduling strategy proposed in this paper.

At the individual EV level, the charging/discharging state of an individual EV changes correspondingly according to the power control signals from the self-scheduling strategy of the VPP.

3. Self-scheduling strategy of VPP

Before establishing the responsive model of the VPP, the response process of EVs is decomposed into four response modes shown in Fig. 2. According to the three states of a battery: discharge, charging and idle, and then the four response modes are summarized as mode I, II, III and IV, respectively.

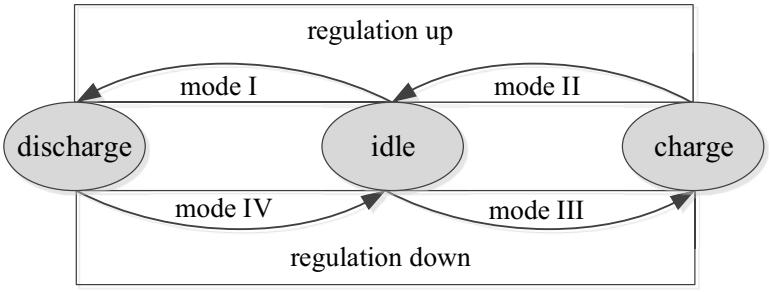

Fig. 2. Response modes of a single EV

3.1. A general model for VPP with EVs

Taking the slow charging mode for EV_i as an example, the energy storage characteristics of a single EV are shown in Fig. 3. The shading part is the operation area of the EV_i in the process of V2G [21].

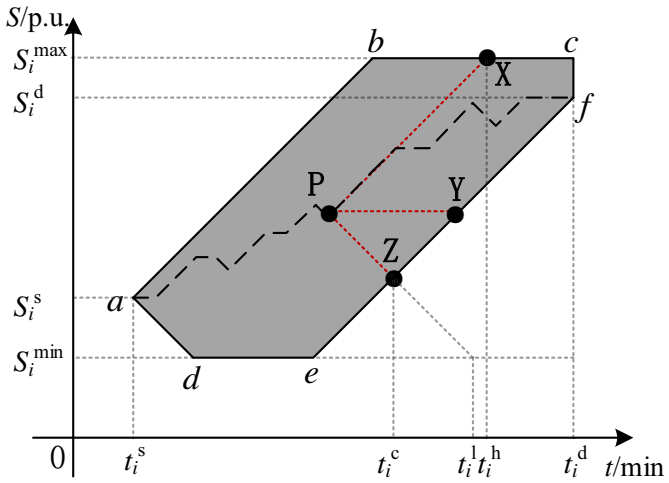

Fig. 3. Energy storage characteristics of an EV

Take EV_i as an example, EV_i is assumed to be connected to the power grid at $t_{i,s}$ and disconnected at the time $t_{i,d}$. In order to prevent the aging of batteries, $S_{i,\max}$ and $S_{i,\min}$ are set as the SOC upper and lower limits of EV_i, respectively. EV_i starts to charge at the rated power P_i^m immediately after it is connected to the grid at $t_{i,s}$, and switches to an idle state when the SOC reaches $S_{i,\max}$, corresponding to the boundary *a*-*b*-*c* in Fig. 3. On the contrary, the boundary *a*-*d*-*e* indicates that EV_i is discharged at P_i^m since $t_{i,s}$, and stops discharging when the SOC is lower than $S_{i,\min}$. In addition, in order to ensure that the SOC of EV_i can reach its minimum SOC ($S_{i,d}$) required by the EV user when leaving the grid, the boundary *e*-*f* indicates that the battery needs to be charged compulsively before travelling.

Without participating any response mode, the charging state of an EV at time t (see $\sigma(t)$ in (1)) is defined in Eq. (1).

$$\sigma(t) = \begin{cases} 1, \ 0 \le S_i(t) < S_{i,d} & t \in [t_{i,s}, \ t_{i,d}] \\ 0, \ S_{i,d} \le S_i(t) < S_{i,\max} & t \in [t_{i,s}, \ t_{i,d}] \end{cases}, \tag{1}$$

where: $S_i(t)$ is the battery SOC of EV_i at time t; $\sigma(t)$ equals to '0' and '1' means the EV is in idle and charging states, respectively. When participating in the power scheduling process, the $\sigma(t)$ will be adjusted according to the response mode depicted in Fig. 2. However, when the EV is in the discharging state, $\sigma(t)$ is set to be '-1'.

When evaluate the response capability of a single EV at a specific time, it will be determined considering the $\sigma(t)$, $S_{i,\max}$, and $S_{i,\min}$ at the same time. The response capability of a single EV for participating the four response modes are shown in Eqs. (2)–(4).

$$P_i^{u,\mathrm{I}}(t) = \begin{cases} P_i^m, & \sigma(t) = 0 \\ 0, & \text{others} \end{cases}, \tag{2}$$

$$P_i^{u,\mathrm{II}}(t) = \begin{cases} P_i^m, & \sigma(t) = 1 \\ 0, & \text{others} \end{cases}, \tag{3}$$

$$P_i^{u,\mathrm{III}}(t) = \begin{cases} -P_i^m, & \sigma(t) = 0, \quad S_i(t) < S_{i,\max} \\ 0, & \text{others} \end{cases}. \tag{4}$$

In general, it is assumed that the dotted curve a-P in Fig. 3 represents the operating state of EV_i after it is connected to the power grid. Taking the operation point P as the current operation state, we can get the fastest charging process PX, idle process PY and the fastest discharge process PZ.

In a given scheduling period $[nT, \ (n{+}1)T]$, the time t_i^c when EV_i reaches the forced charging power is obtained by Eq. (5).

$$t_i^c = \frac{\left(\dfrac{Q_i(S_i(nT) - S_{i,d})\eta^d}{P_i^m} + nT\eta^c\eta^d + t_{i,d} \right)}{(\eta^c\eta^d + 1)}, \tag{5}$$

where Q_i is the battery capacity and η^c, η^d represent the charging and discharging efficiency, respectively.

The time t_i^l can be obtained by Eq. (6), when EV_i reaches the lower bound of the controllable region.

$$t_i^l = \frac{Q_i \left(S_i(nT) - S_{i,\min}\right) \eta^d}{P_i^m} + nT. \tag{6}$$

Based on the above analysis, the available response capacity of the VPP is show in Eq. (7).

$$\begin{cases} \overline{P}^{u}(t) = \sum_{i=1}^{N} \left(P_i^{u,\mathrm{I}}(t) + P_i^{u,\mathrm{II}}(t) \right) \\ \underline{P}^{u}(t) = \sum_{i=1}^{N} P_i^{u,\mathrm{III}}(t) \end{cases}, \tag{7}$$

where N is the number of EVs in the VPP.

However, the $S_i(t)$ has close relationship with the response mode in the time $[t_i^s,\ t]$. The Eqs. (8)–(10) are used to amend the available response capability in a scrolling manner.

$$\begin{cases} S_i(t) = \begin{cases} S_i\left(t_{i,s}\right) + \Delta S_i, & t_{i,s} \le t \le t_{i,d} \\ 0, & \text{others} \end{cases} \\ \Delta S_i = \dfrac{1}{Q_i} \displaystyle\int_{t_{i,s}}^{t} \left(P_i^{uc}(t) - P_i^{\mathrm{II}}(t) - P_i^{\mathrm{III}}(t) \right) \eta^c - \left(P_i^{\mathrm{I}}(t) + P_i^{\mathrm{IV}}(t) \right) \dfrac{1}{\eta^d} \mathrm{d}t \end{cases}, \tag{8}$$

$$P_i^{uc}(t) = P_i^m \sigma(t), \tag{9}$$

$$P_i^k(t) = \begin{cases} P_i^m, & k = \mathrm{I},\ \mathrm{II} \\ -P_i^m, & k = \mathrm{III},\ \mathrm{IV} \\ 0, & \text{without-participation} \end{cases}, \tag{10}$$

where: P_i^{uc} is the charging power of EV_i without participating any response mode; P_i^{IV} is the response power when participating in mode IV.

3.2. The definition of EV queueing index in a VPP

Each EV connected to the power system can respond quickly enough to the scheduling power from the power system. Such actions may lead to a rapid variation in the battery responsiveness, and even unable to respond continuously. Take mode I in Fig. 2 as an example, the maximum time that an EV can sustain an excessive response during the scheduling period is defined as the response time margin (RTM) under this response mode, as shown in Eq. (11).

$$RTM_i^n = \begin{cases} 0, & nT \notin [t_{i,s},\ t_{i,d}] \ \text{ and } \ (n+1)T \notin [t_{i,s},\ t_{i,d}] \\ T, & \left\{ t_{i,s},\ t_i^l,\ t_i^c,\ t_{i,d} \right\} \not\subset (nT,\ (n+1)T] \\ \min\left(t_i^l,\ t_i^c,\ t_{i,d},\ (n+1)T \right) - \max\left(t_{i,s},\ nT \right), & \text{otherwise} \end{cases}. \tag{11}$$

As shown in Eq. (11), in a given scheduling period, the $RTM_i^n \in [0,\ T\ ]$. When the VPP participates in the optimal scheduling process of the power system, the larger the RTM_i^n, the longer the response time that the EV can sustain. This means that the EV with a large RTM_i^n will be selected with a high priority to participate in the response process. However, in the $[nT,\ (n+1)T\ ]$ period, there may be multiple EVs whose RTM_i^n is equal to T, and only the single RTM

index will not provide a clear priority sequence among the EVs to response to the power system. Therefore, an index called the state of charge margin (SOCM) is also defined in this section.

The SOCM index is defined as shown in Eq. (12) [22].

$$\mathrm{SOCM}_i^n = \begin{cases} \dfrac{S_{i,d} - S_i(nT)}{S_{i,d} - S_i^{\min}}, & \Delta P^n \le 0 \\ \dfrac{S_i(nT) - S_i^{\min}}{S_{i,d} - S_i^{\min}}, & \Delta P^n > 0 \end{cases}, \tag{12}$$

$$\Delta P^n = \begin{cases} P^*(n), & n = 1 \\ P^*(n+1) - P^*(n), & n > 1 \end{cases}, \tag{13}$$

where: $P^*(n)$ is the response power demand just before the $[nT, (n+1)T]$ time period; ΔP^n denotes the power variation of the response power at the $[nT, (n+1)T]$ period compared with the previous time period. ΔP^n is used as the response power variation demand of the VPP. A negative value means that the VPP needs to reduce its power output, while a positive value means that the VPP needs to increase its power output.

When the VPP needs to reduce its power output, the EV_i with a high SOCM, will stop discharging, and even starts to charge. In contrary, when the VPP needs to increase its power output, the EV_i with a higher SOCM, will stop charging, and even starts to discharge.

3.3. Self-scheduling strategy of the VPP

When the $\Delta P(t)$ is determined at the control centre level, the self-scheduling strategy of the VPP is used to allocate the power to each EV in the VPP. The specific steps of self-scheduling strategy of the VPP are described as follows:

1. For a given time period $[nT, (n+1)T]$, according to the states of the VPP, the response capability of the VPP is evaluated using Eq. (7).

2. The EVs in the VPP are divided into four control groups according to the four response modes depicted in Fig. 1. A single EV can participate in multiple modes at the same time. There is an intersection between different groups.

3. When the power response request of the VPP from the power system is determined at the control centre level, it will be then allocated to the specific EVs in the VPP with a pre-defined queuing discipline.

At the first stage, each EV controlled group is arranged in the order of the RTM, from large to small. For EVs with the same RTM, the corresponding priority sequence of each group is obtained by referring to the descending order of the SOCM. Using this discipline, the EVs are sorted to generate a priority sequence of responsive EVs for the VPP.

***Scenario I*:** when the VPP output is required to be up-regulated, the priority sequence generated by the response mode group from a charging state to an idle state is considered firstly. When all EVs stop charging and still cannot satisfy the response power request curve, the "idle"→"discharge" group needs to be supplemented.

***Scenario II*:** when the output of VPP is required to be down-regulated, the "discharge"→"idle" group is preferentially selected to generate a priority sequence. When all EVs are charged and the response curve cannot be satisfied, the "idle"→"charge" group should be considered.

In each scenario, according to the response power request, the EVs at the front end of the sequence is selected to adjust the charge/discharge power directly.

4. As is shown in Eq. (14), according to the response power from the power system, and based on the priority sequence step III, the minimum positive integer is used as the number (N_o) of response EVs in the VPP.

$$\begin{cases} \sum_{i=1}^{N_o} P_i^{\mathrm{II}}(t) \geq \Delta P^n, \quad 0 \leq \Delta P^n \leq \sum_{i=1}^{N} P_i^{\mathrm{II}}(t) \\ \sum_{i=1}^{N} P_i^{\mathrm{II}}(t) + \sum_{i=1}^{N_o} P_i^{\mathrm{I}}(t) \geq \Delta P^n, \quad \sum_{i=1}^{N} P_i^{\mathrm{II}}(t) \leq \Delta P^n \\ \sum_{i=1}^{N_o} P_i^{\mathrm{IV}}(t) \leq \Delta P^n, \quad \sum_{i=1}^{N} P_i^{\mathrm{IV}}(t) \leq \Delta P^n < 0 \\ \sum_{i=1}^{N} P_i^{\mathrm{IV}}(t) + \sum_{i=1}^{N_o} P_i^{\mathrm{III}}(t) \leq \Delta P^n, \quad \Delta P^n \leq \sum_{i=1}^{N} P_i^{\mathrm{IV}}(t) \end{cases} . \tag{14}$$

For a comparison purpose, an ID order control strategy for the EVs in the VPP is introduced. In the ID order control strategy, the EV VPP is numbered according to the order of a connecting EV charger. Response capability is calculated in turn until the VPP is composed of the first N_o+11 EVs, which can satisfy the response power demand. Finally, the control scheme of charging/discharging power of N_o of EVs is obtained.

4. Simulation analysis

4.1. Scenario setup

Considering that EVs charging periods for different purposes show great differences, it will hence have critical influences on the results of calculation examples. According to statistics on registered vehicles in the UK, private commuter vehicles, private non-commuter vehicles (generally characterized by those retired from work or who are unemployed) and corporate vehicles account for 61%, 30% and 9% of the EVs market for three different purpose, respectively [23]. According to the above market share, this case takes the VPP composed of 300 EVs as an example to verify the proposed VPP self-scheduling strategy. According to different vehicle traffic uses, the start-finish time distribution of EVs daily travel is shown in literature [24]. The distributions of other EV parameters, such as the battery capacity, the charging/discharging power, the charging/discharging efficiency, the initial SOC, and the demand SOC are shown in literature [9].

Each parameter of an individual EV can be extracted from the distributions in literatures [24] and [9]. Then each EV is simulated and its response characteristics can be according with the obtained general model for the VPP with EVs. An EV is assumed to start to charge as soon as the EV plugs into the power grid, and the charging process will not be disturbed until the demanded SOC is reached or the control signal is received. Then specific steps of self-scheduling strategy of the VPP can be conducted with all simulated EVs in the VPP.

In addition, in order to realize the simulation of the control effect of the VPP participating in the system scheduling, this paper set the scheduling time interval as 1h, and assumed that the scheduling power demand of the VPP issued by the system operator was shown as the dotted line of Fig. 4. Finally, the change of response requirement ΔP^n corresponding to the model is obtained, as shown by the solid line of Fig. 4.

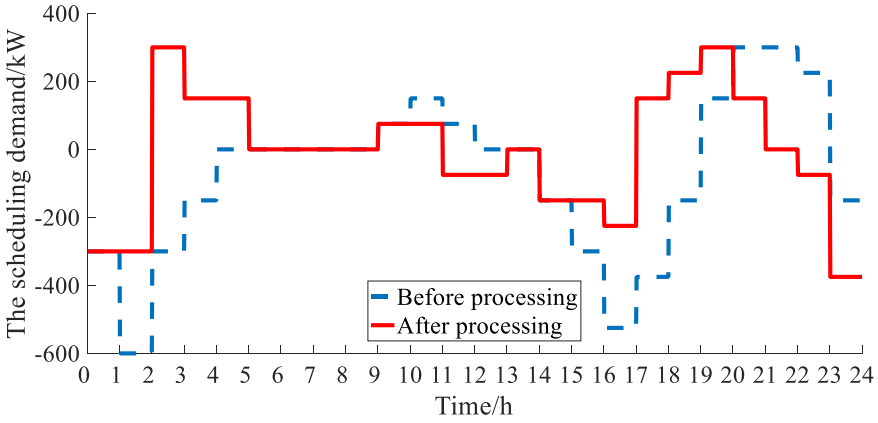

Fig. 4. The scheduling power demand of VPP

4.2. Results analysis

According to the four response modes, the VPP was divided into different groups, and the RTM and SOCM indexes were calculated, respectively. As shown in Fig. 5, compared with the ID order control strategy, the self-scheduling strategy can significantly reduce the number of controlled EVs. Fig. 5 also shows the number distribution of controlled EVs under different response modes. By the parameters optimal selection of the RTM and SOCM, the number of EVs participating in the response mode II (i.e. "charging"→"idle" response) is significantly reduced. Even compared with the ID order control strategy, the VPP does not have to discharge to the power grid in multiple periods.

To further explain why the proposed self scheduling strategy decreases the number of controlled EVs during multiple time periods, more simulation results have been added to further illustrate the effectiveness of the RTM and SOCM indexes in the proposed self scheduling strategy. Simulation results about the RTM and SOCM during the 19:00–22:00 time period are shown in Fig. 6. It is noteworthy that the EVs have significant differences in the RTM and SOCM as the SOC levels are uneven after one daytime travels. Thus it is reasonable to develop the priority method for regulating up or down EVs based on the differences of EVs in the RTM and SOCM.

Then, considering the RTM and SOCM indices, the results of EVs ranking in the above period are shown in Fig. 7, and the data label in the figure is an EV ID number. The RTM and SOCM indices of each EV need to be updated and calculated continuously in each scheduling period. Different from ID order control strategy, the self-scheduling control strategy firstly ranks the EVs in descending order according to the RTM. When the RTM is equal, it further defines the higher priority level of the larger SOCM, participates in response preferentially on the basis

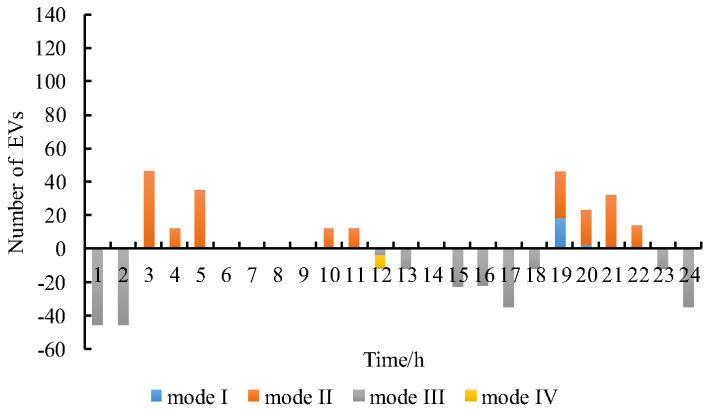

(a) Self scheduling strategy

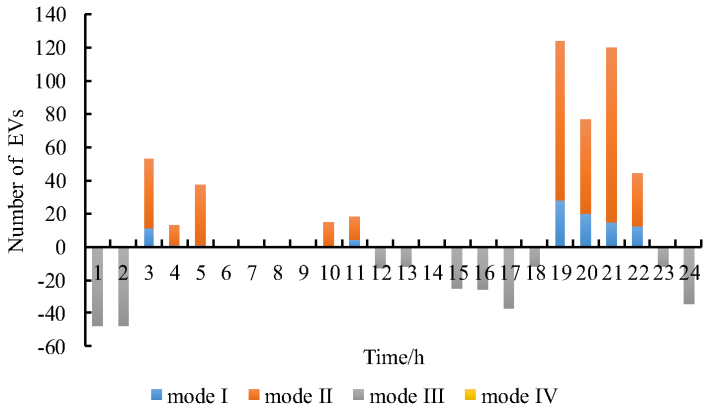

(b) ID order control strategy

Fig. 5. The number distribution of controlled EVs under different response modes

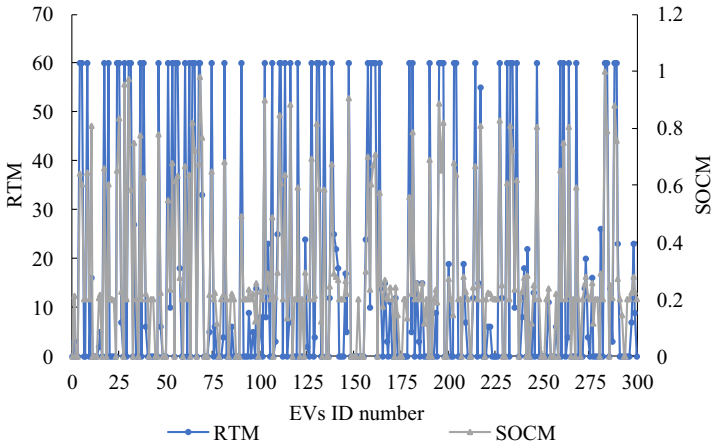

Fig. 6. Simulation results of RTM and SOCM

of considering both the scheduling power and user travel demand. Finally it obtains the decision-making conclusion when the VPP participates in multi-time-scale scheduling. The EV with a higher priority has a higher RTM and correspondingly has a longer available period for power control. Thus, the proposed self scheduling strategy decreases the number of controlled EVs as shown in Fig. 5.

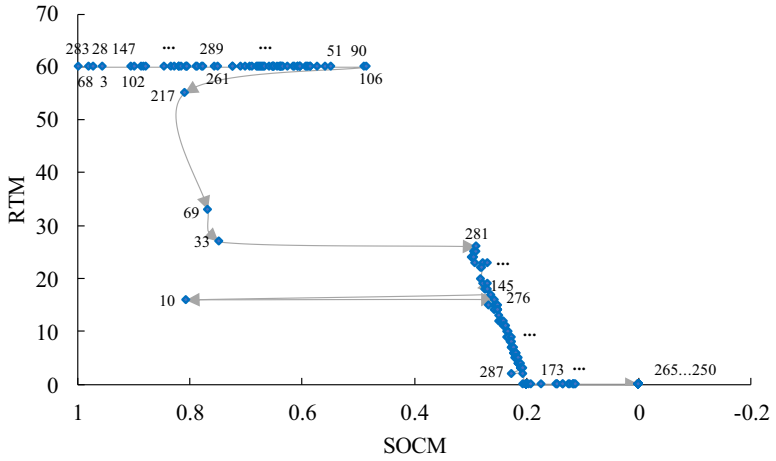

Fig. 7. The sequencing results of each EV

The average SOC distribution of all EVs is shown in Fig. 8. Compared with the ID order control strategy, the proposed self scheduling strategy prevents the SOC value of an EV reaching too high or too low to some degree. The proposed strategy makes the distribution of the SOC values of EVs more centralized. This is because that the EVs with the higher RTM and SOCM

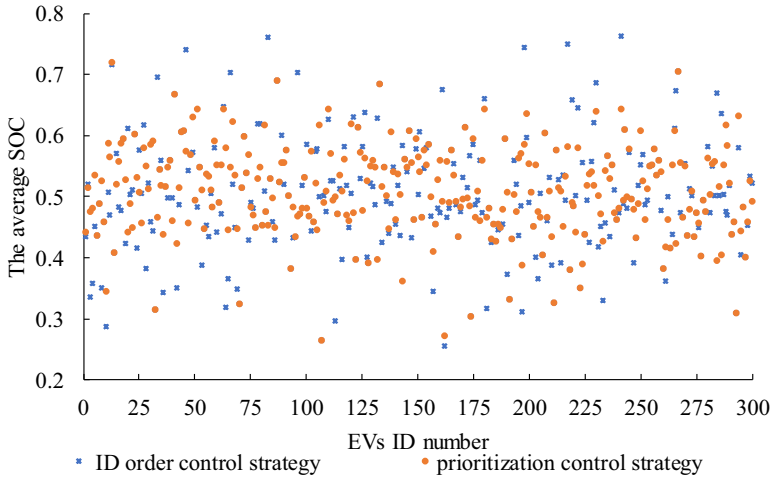

Fig. 8. The average SOC distribution of each EV

have the priority to be controlled with the proposed self scheduling strategy. For an EV in the charging state with a low SOC value, it has a small SOCM for regulating up, and the EV locates at the bottom of the priority list when regulating up. Thus, the charging process of this EV has the lower probability to be disturbed. For an EV in the charging state with a high SOC value, it has a high SOCM for regulating up, and the EV locates at the top of the priority list when regulating up. Thus, the charging process of this EV has the higher probability to switch to idle and even discharging.

5. Conclusions

This paper proposes a self-scheduling strategy of a VPP considering the RTM and SOCM selection indexes method. Comparable results validate the effectiveness of the proposed self-scheduling strategy of the VPP. The conclusions are summarized as follows:

1) The RTM parameter is used to prioritize the EV with long duration response time, reduce the number of controlled EV and reduce the switching frequency of charging and discharging states in the VPP. The SOCM parameter takes the limitation and demand value of the SOC as reference to realize that when the VPP output is up-regulated (down-regulated). An EV with a smaller difference from the lower limit of the SOC (demand value of SOC) should be selected to stop charging (discharging) or even start discharging (charging) to avoid the local high or low average SOC. The proposed RTM and SOCM indices provide a good metric for estimating the available response capacity under different response modes during the grid-connecting period.

2) On the basis of group division of the VPP, the EVs are sorted according to the selected indexes, and the priority sequences are generated. Finally, the controlled EVs are determined according to the issued scheduling power. The VPP self-scheduling strategy can meet the scheduling requirements and ensure the comfort of EV users. Thus, the proposed self-scheduling strategy considering the RTM and SOCM effectively decreases the number of the controlled EVs when responding to the power grid.

In actual applications, switching to DS incurs extra battery degradation. With a low charging/discharging rate, the main factor that impacts battery degradation is the total processed energy [25, 26]. Thus, the extra battery degradation caused by switching to DS is set to be approximately proportional to the discharged energy. As an EV aggregator does not own EV batteries, it needs to compensate EVs for the extra battery degradation. Due to different preferences of EVs, the expected compensation prices of different EVs for per unit discharged energy are various. By referring to the electricity market, the EV aggregator is assumed to contract and trade with EV users at the same clearing price for the extra battery degradation compensation. The EV aggregator has the authority to implement the four response modes with the contracted EVs. All EVs are treated equally and the profits of EVs are ensured. The clearing price directly impacts the participation rate of EVs for the regulation service.

References

[1] Chen C., Guo C., Man Z. *et al.*, *Control strategy research on frequency regulation of power system considering Electric vehicles*, 2016 IEEE PES Asia-Pacific Power and Energy Engineering Conference (2016).

[2] Chen Y.K., Lin C.H., Wang W.C., *The conversion of biomass into renewable jet fuel*, Energy, vol. 201, pp. 1–9 (2020).

[3] Schuller A., Dietz B., Flath C.M. *et al.*, *Charging strategies for battery electric vehicles: Economic benchmark and V2G potential*, IEEE Transactions on Power Systems, vol. 29, no. 5, pp. 2014–2022 (2014).

[4] Xia S., Bu S., Luo X. *et al.*, *An autonomous real time charging strategy for plug-in electric vehicles to regulate frequency of distribution system with fluctuating wind generation*, IEEE Transactions on Sustainable Energy, vol. 9, no. 2, pp. 511–524 (2017).

[5] Mroczek B., Kołodyńska A., *The V2G Process with the Predictive Model*, IEEE Access, vol. 8, pp. 86947–86956 (2020).

[6] Zhang H., Hu Z., Xu Z., Song Y., *Evaluation of achievable vehicle-to-grid capacity using aggregate PEV model*, IEEE Transactions on Power Systems, vol. 32, no. 1, pp. 784–794 (2017).

[7] Ko K., Han S., Dan K.S., *Performance-Based Settlement of Frequency Regulation for Electric Vehicle Aggregators*, IEEE Transactions on Smart Grid, vol. 9, no. 2, pp. 866–875 (2018).

[8] Vagropoulos S.I., Kyriazidis D.K., Bakirtzis A.G., *Real-Time Charging Management Framework for Electric Vehicle Aggregators in a Market Environment*, IEEE Transactions on Smart Grid, vol. 7, no. 2, pp. 948–957 (2016).

[9] Wang M., Mu Y., Shi Q. *et al.*, *Electric vehicle aggregator modeling and control for frequency regulation considering progressive state recovery*, IEEE Transactions on Smart Grid, Early Access (2020).

[10] Cao Y., Tong W., Omprakash K. *et al.*, *An EV Charging Management System Concerning Drivers' Trip Duration and Mobility Uncertainty*, IEEE Transactions on Systems Man and Cybernetics Systems, vol. 48, no. 4, pp. 596–607 (2017).

[11] Zheng J., Wang X., Men K. *et al.*, *Aggregation model-based optimization for electric vehicle charging strategy*, IEEE Transactions on Smart Grid, vol. 4, no. 2, pp. 1058–1066 (2013).

[12] Wang M., Mu Y., Jai H. *et al.*, *Active power regulation for large-scale wind farms through an efficient power plant model of electric vehicles*, Applied Energy, vol. 185, pp. 1673–1683 (2017).

[13] Meng J., Mu Y., Jia H. *et al.*, *Dynamic frequency response from electric vehicles considering travelling behavior in the Great Britain power system*, Applied Energy, vol. 162, pp. 966–979 (2016).

[14] Kaur K., Singh M., Kumar N., *Multiobjective optimization for frequency support using electric vehicles: An aggregator-based hierarchical control mechanism*, IEEE System Journal, vol. 13, no. 1, pp. 771–782 (2019).

[15] Li G., Huang Y., Bie Z., *Reliability Evaluation of Smart Distribution Systems Considering Load Rebound Characteristics*, IEEE Transactions on Sustainable Energy, vol. 9, no. 4, pp. 1713–1721 (2018).

[16] Zhe W., Yue L., Lin C., *Electric Vehicle Charging Scheme for a Park-and-Charge System Considering Battery Degradation Costs*, IEEE Transactions on Intelligent Vehicles, vol. 3, no. 3, pp. 361–373 (2018).

[17] Zhang Z., Dong K., Pang X. *et al.*, *Research on the EV charging load estimation and mode optimization methods*, Archives of Electrical Engineering, vol. 68, no. 4, pp. 831–842 (2019).

[18] Li C.T., Ahn C., Peng H. *et al.*, *Synergistic control of plug-in vehicle charging and wind power scheduling*, IEEE Transactions on Power Systems, vol. 28, no. 2, pp. 1113–1121 (2013).

[19] Xu S., Yan Z., Feng D. *et al.*, *Decentralized charging control strategy of the electric vehicle aggregator based on augmented Lagrangian method*, International Journal of Electrical Power and Energy Systems, vol. 104, pp. 673–679 (2019).

[20] Jian L., Zheng Y., Shao Z., *High efficient valley-filling strategy for centralized coordinated charging of large-scale electric vehicles*, Applied Energy, vol. 186, pp. 46–55 (2017).

[21] Wang M., Mu Y., Jiang T. *et al*., *Load curve smoothing strategy based on unified state model of different demand side resources*, Journal of Modern Power Systems and Clean Energy, vol. 6, no. 3, pp. 540–554 (2018).

[22] Qi Y., Wang D., Jia H. *et al*., *Research on demand response for thermostatically controlled appliances based on normalized temperature extension margin control strategy*, Proceedings of the CSEE, vol. 21 (2015).

[23] Qian K., Zhou C., Allan M. *et al*., *Modeling of load demand due to EV battery charging in distribution systems*, IEEE Transactions on Power Systems, vol. 26, no. 2 pp. 802–810 (2011).

[24] Wang M., Mu Y., Jai H. *et al*., *A preventive control strategy for static voltage stability based on an efficient power plant model of electric vehicles*, Journal of Modern Power Systems and Clean Energy, vol. 3, no. 1, pp. 103–113 (2015).

[25] Zhou C., Qian K., Allan M. *et al*., *Modeling of the cost of EV battery wear due to V2G application in power systems*, IEEE Transactions on Power Electronics, vol. 26, no. 4, pp. 1041–1050 (2011).

[26] Liu C., Wang X., Wu X. *et al*., *Economic scheduling model of microgrid considering the lifetime of batteries*, IET Generation, Transmission and Distribution, vol. 11, no. 3, pp. 759–767 (2017).